

A multigroup spline approximation in extended kinetic theory

This article has been downloaded from IOPscience. Please scroll down to see the full text article.

2002 J. Phys. A: Math. Gen. 35 8673

(<http://iopscience.iop.org/0305-4470/35/41/303>)

View [the table of contents for this issue](#), or go to the [journal homepage](#) for more

Download details:

IP Address: 171.66.16.109

The article was downloaded on 02/06/2010 at 10:33

Please note that [terms and conditions apply](#).

A multigroup spline approximation in extended kinetic theory

C Ertler, F Schürer and W Koller

Institute for Theoretical Physics, Technical University of Graz, Austria

E-mail: ertler@itp.tu-graz.ac.at and schuerer@itp.tu-graz.ac.at

Received 8 May 2002

Published 1 October 2002

Online at stacks.iop.org/JPhysA/35/8673

Abstract

We introduce an extended linear Boltzmann equation governing the distribution function of charged particles which scatter inelastically with resting heavy background particles. The appearing collision integral is closely connected to a simplified description of the electron–phonon interaction in semiconductors. The particle conservation and the balance equations of momentum and energy are discussed in the Lorentz gas limit. By applying a multigroup spline approximation combined with a P_1 -approximation for the angle dependence of the distribution function, the Boltzmann equation is reduced to a system of differential equations. This approach incorporates external forces in a natural way. The multigroup equations are solved numerically for different scenarios.

PACS numbers: 02.60.Nm, 51.10.+y, 05.20.Dd

1. Introduction

The Boltzmann equation is an integro-differential equation, which can be solved rigorously only in simple cases. Therefore, it is necessary to find approximations to obtain at least numerically solvable equations. One possibility, known as discrete velocity models, is to allow the particles to attain only a certain set of velocities. However, in these models it is impossible to handle external forces without further approximations. To compensate for this disadvantage, we propose a continuous multigroup approach based on the method of weighted residuals [1] in this work. Indeed, multigroup approaches are known in the field of transport theory [2] as simple and fruitful ways to treat the speed variable v . Recently, the standard multigroup method originally devised for neutron transport was generalized for nonlinear extended Boltzmann equations [3]. This method, however, brings

in additional unknowns by integrating the derivatives of the distribution function with respect to velocity, which stem from the force term in the Boltzmann equation. To overcome this difficulty, a kind of overlapping multigroup approach which allows an exact integration by parts within each group is developed [4]. This development, however, results in a more complex structure of the multigroup equations. To obtain a simpler system of multigroup equations, we interpolate the velocity dependence of the distribution function by a sum of Legendre polynomials (splines) within each group in this paper. When deriving the multigroup equations, we can take advantage of the orthogonality relations of Legendre polynomials.

We apply this multigroup spline method to a linear extended Boltzmann equation which is derived for the following physical situation. A system of two kinds of charged particles, say A (mass m_A) and B (mass m_B), can interact via inelastic binary collisions. The particles B are assumed to be much heavier than the other ones ($m_B \gg m_A$) and are at rest for all times. This is reasonable because after a collision with a light particle A, a particle B stays practically at rest. These assumptions are known as the Lorentz gas approximation. Moreover, we assume that it is possible that the light test particles excite the particles B to a higher energy level by inelastic interaction. We will denote the excited particles by B^* . The whole system should be embedded in a heat bath which impresses a given constant temperature T . Consequently, it follows from the Boltzmann distribution for a canonical ensemble that the particle density of the excited particles B^* is given by

$$n_{B^*} = n_B \exp\left(-\frac{\Delta E}{k_b T}\right) \quad (1)$$

where ΔE denotes the energy difference between the ground state and the excited energy level and k_b is the Boltzmann constant. The interaction due to the electric field which is caused by the charged particles themselves is taken into consideration by means of a force term within the Boltzmann equation. Hence, the force term of the Boltzmann equation is constituted by the sum of a 'real' external force and the self-consistent field which results from the Poisson equation. The Poisson equation governs the electric potential due to the charge distribution of the species A and B. The only interesting elementary processes which enter in the collision integral are then the inelastic collisions with heavy particles. In other words, collective long-range interactions are taken into consideration by the self-consistent field, whereas short-range binary collisions are described by the collision integral. In our model, only the number of particles is conserved, because the light test particles can exchange energy and momentum with the background gas. To sum up, the light particles move in a heavy background gas which is always in thermal equilibrium. This model is closely connected to the problem of electron transport in semiconductors [5], where the phonons are considered as a background gas and the electrons of the conduction band are identified with the light test particles A.

This paper is organized as follows. After this introduction, the extended linear Boltzmann equation concerning the physical situation mentioned above is presented and its macroscopic properties are discussed in section 2. The multigroup spline approach is introduced and discussed in section 3. In view of the numerical simulations, we confine ourselves to a linear anisotropy approximation for the distribution function, the so-called P_1 -approximation. This means that the expansion of the angular dependence of the distribution function in terms of spherical harmonics is truncated after the first-order term. Due to this assumption, the validity of our model is restricted to weak external forces. Finally, section 4 illustrates the numerically obtained solutions to the multigroup equations for different physical scenarios.

2. Macroscopic properties

The Boltzmann equation for the test particle distribution function f which corresponds to the physical problem sketched in the introduction reads [6]

$$\frac{\partial f}{\partial t} + \mathbf{v} \cdot \frac{\partial f}{\partial \mathbf{r}} + \frac{\mathbf{F}}{m} \cdot \frac{\partial f}{\partial \mathbf{v}} = \mathcal{C}[f] \quad (2)$$

where $m = m_A$. The inelastic collision integral $\mathcal{C}[f]$ is given by

$$\begin{aligned} \mathcal{C}[f] = & \int_{S^2} d\Omega' \frac{(v_-)^2}{v} \sigma_{\text{de}}(v_- \Omega', \Omega) n_{B^*} f(v_- \Omega') + \int_{S^2} d\Omega' \frac{(v_+)^2}{v} \sigma_{\text{ex}}(v_+ \Omega', \Omega) n_B f(v_+ \Omega) \\ & - \int_{S^2} d\Omega' v \sigma_{\text{ex}}(v \Omega, \Omega') n_B f(v \Omega) - \int_{S^2} d\Omega' v \sigma_{\text{de}}(v \Omega, \Omega') n_{B^*} f(v \Omega). \end{aligned} \quad (3)$$

Elastic scattering is not considered here, since inelastic collisions are assumed to be dominant. The distribution function $f(\mathbf{r}, \mathbf{v}, t)$ depends on position \mathbf{r} , velocity \mathbf{v} and time t . We consider only the Lorentz force

$$\mathbf{F} = e(\mathbf{E} + \mathbf{v} \times \mathbf{B}) \quad (4)$$

due to an electromagnetic field, where e denotes the charge of a test particle, \mathbf{E} is the electric field and \mathbf{B} the magnetic induction. The particle density of the heavy, resting particles B in the ground state (excited state B*) is denoted by n_B (n_{B^*}). We decompose the velocity vector $\mathbf{v} = v\Omega$ in its modulus v and angular part Ω . The integration on the right-hand side of equation (3) extends over the two-dimensional unit sphere S^2 . Moreover, we introduce the abbreviations

$$v_{\pm} = \sqrt{v^2 \pm \varepsilon^2} \quad \varepsilon^2 = \frac{2\Delta E}{m} \quad (5)$$

because the test particle's velocity v changes to v_{\pm} by inelastic collisions and the threshold ε is related to the energy gap ΔE between the ground state and excited state of the background particles. The cross sections σ_{ex} and σ_{de} refer to the excitation and de-excitation processes, respectively. They are linked by the microreversibility condition

$$v^2 \sigma_{\text{ex}}(v \Omega, \Omega') = (v_-)^2 \sigma_{\text{de}}(v_- \Omega', \Omega) \quad v \geq \varepsilon. \quad (6)$$

Moreover, we define

$$\sigma_{\text{ex}}(v \Omega, \Omega') = 0 \quad \text{for } v < \varepsilon \quad (7)$$

since for $v < \varepsilon$ the light particles do not have enough energy to excite a heavy particle.

The physical meaning of the terms in the collision integral can be easily understood. By virtue of the first two terms, particles with velocity v are gained by upscattering due to de-excitation processes and by downscattering due to excitation processes. The last two terms describe the corresponding loss events. For convenience, we introduce the following abbreviations

$$\begin{aligned} f &= f(\mathbf{v}) & f^+ &= f(v_+ \Omega') & f^- &= f(v_- \Omega') \\ \sigma &= \sigma_{\text{ex}}(v \Omega, \Omega') & \sigma^+ &= \sigma_{\text{ex}}(v_+ \Omega', \Omega) & \sigma^- &= \sigma_{\text{ex}}(v_- \Omega', \Omega) \end{aligned} \quad (8)$$

and

$$\mathbf{a} = \frac{e}{m} \mathbf{E} \quad \mathbf{b} = \frac{e}{m} \mathbf{B}. \quad (9)$$

Hence, equation (2) reads

$$\frac{\partial f}{\partial t} + \mathbf{v} \cdot \frac{\partial f}{\partial \mathbf{r}} + (\mathbf{a} + \mathbf{v} \times \mathbf{b}) \cdot \frac{\partial f}{\partial \mathbf{v}} = \mathcal{C}[f] \quad (10)$$

with the collision integral

$$\mathcal{C}[f] = \frac{1}{v} \int d\Omega' [n_B v_+^2 \sigma^+ f^+ + n_{B^*} v^2 \sigma f^- - f(n_B v^2 \sigma + n_{B^*} v_+^2 \sigma^+)] \quad (11)$$

simplified by using the microreversibility condition. For further calculations, we assume $\sigma(v\Omega, \Omega') = \sigma(v, \Omega \cdot \Omega')$, which means that the cross section depends only on the initial speed v and the angle $\theta = \arccos(\Omega \cdot \Omega')$ between the initial and final velocity of the interaction.

The inelastic collisions drive the test particles towards an equilibrium distribution which is a solution to the equation

$$\mathcal{C}[f] = 0. \quad (12)$$

It can be shown [6] that the equilibrium for our special collision integral is mathematically exhausted by the class of functions

$$f(v\Omega) = C(v^2) \exp\left(-\frac{mv^2}{2k_b T}\right) \quad \text{with} \quad C(v^2 + \varepsilon^2) = C(v^2). \quad (13)$$

Choosing $C(v^2) = \text{const}$, we obtain the standard Maxwellian

$$f(v\Omega) = n \left(\frac{m}{2\pi k_b T}\right)^{\frac{3}{2}} \exp\left(-\frac{mv^2}{2k_b T}\right) \quad (14)$$

where $n = \int f d\mathbf{v}$ is the particle density of species A. This means that if there is no diffusion ($\frac{\partial f}{\partial \mathbf{r}} = 0$) and no external forces are applied, our light particles will be found in a Maxwellian state at the given background temperature.

Since the distribution function represents the expected number of particles at position \mathbf{r} and velocity \mathbf{v} , we can generally find the value of a macroscopic quantity $Q(\mathbf{r}, t)$ corresponding to the velocity-dependent microscopic quantity $q(\mathbf{v})$ by

$$Q(\mathbf{r}, t) = \int_{R^3} q(\mathbf{v}) f(\mathbf{r}, \mathbf{v}, t) d\mathbf{v}. \quad (15)$$

In particular, we define the following macroscopic quantities:

- *particle density*

$$n(\mathbf{r}, t) = \int_{R^3} f(\mathbf{r}, \mathbf{v}, t) d\mathbf{v} \quad (16)$$

- *current density*

$$\mathbf{J}(\mathbf{r}, t) = \int_{R^3} \mathbf{v} f(\mathbf{r}, \mathbf{v}, t) d\mathbf{v} \quad (17)$$

- *momentum flux per unit mass*

$$\{\mathcal{K}(\mathbf{r}, t)\}_{ij} = K_{ij}(\mathbf{r}, t) = \int_{R^3} v_i v_j f(\mathbf{r}, \mathbf{v}, t) d\mathbf{v} \quad (18)$$

- *energy density per unit mass*

$$K(\mathbf{r}, t) = \int_{R^3} \frac{v^2}{2} f(\mathbf{r}, \mathbf{v}, t) d\mathbf{v} = \frac{1}{2} \text{tr} K_{ij} \quad (19)$$

- *energy flux per unit mass*

$$\mathbf{Q}(\mathbf{r}, t) = \int_{R^3} \left(\frac{v^2}{2}\right) \mathbf{v} f(\mathbf{r}, \mathbf{v}, t) d\mathbf{v} \quad (20)$$

where tr denotes the trace of a tensor.

The evolution equations for the macroscopic quantities are obtained by multiplying the Boltzmann equation with the appropriate velocity moments $q(v)$ and integrating it over the whole velocity space. Taking $q(v) = 1$, we obtain the continuity equation

$$\frac{\partial n}{\partial t} + \text{div} \mathbf{J} = 0 \quad (21)$$

which reflects the important physical statement that the number of particles A is conserved in our model. When integrating the collision term, it proves convenient to introduce the total cross section

$$\sigma_0(v) = \int \sigma(v, \boldsymbol{\Omega} \cdot \boldsymbol{\Omega}') \, d\boldsymbol{\Omega} = 2\pi \int_{-1}^1 \sigma(v, \mu) \, d\mu \quad (22)$$

with $\mu = \boldsymbol{\Omega} \cdot \boldsymbol{\Omega}' = \cos \theta$ as well as the average cosine of the scattering angle

$$\langle \mu \rangle(v) = \frac{2\pi}{\sigma_0} \int_{-1}^1 \mu \sigma(v, \mu) \, d\mu = \frac{\sigma_1}{\sigma_0} \quad (23)$$

bearing in mind the useful identity

$$\int \boldsymbol{\Omega} \sigma(v, \boldsymbol{\Omega} \cdot \boldsymbol{\Omega}') \, d\boldsymbol{\Omega} = 2\pi \boldsymbol{\Omega}' \int_{-1}^1 \mu \sigma(v, \mu) \, d\mu = \sigma_1(v) \boldsymbol{\Omega}'. \quad (24)$$

The analogous quantities for the de-excitation cross section σ_{de} are defined in the same way.

The equation of momentum transport is obtained after some algebra by using $q(v) = \mathbf{v}$ as a weight function:

$$\begin{aligned} \frac{\partial \mathbf{J}}{\partial t} + \frac{\partial}{\partial \mathbf{r}} \cdot \mathcal{K} - n\mathbf{a} + \mathbf{b} \times \mathbf{J} = n_{\text{B}} \int_{\varepsilon}^{\infty} d\mathbf{v} v^3 \sigma_0^{\text{ex}}(v) [v_- \langle \mu_{\text{ex}} \rangle(v) - v] \int d\boldsymbol{\Omega} \boldsymbol{\Omega} f \\ + n_{\text{B}^*} \int_0^{\infty} d\mathbf{v} v^3 \sigma_0^{\text{de}}(v) [v_+ \langle \mu_{\text{de}} \rangle(v) - v] \int d\boldsymbol{\Omega} \boldsymbol{\Omega} f. \end{aligned} \quad (25)$$

The two terms on the right-hand side of this equation are the rate of change of the current density due to collisions. This is also obvious from a heuristic point of view. The number of particles A (with velocity \mathbf{v} in $d\mathbf{v}$) which change their velocity by exciting particles B per unit time is given by

$$dN_{\text{ex}} = \sigma_0^{\text{ex}}(v) n_{\text{B}} f(v\boldsymbol{\Omega}) v \, d\mathbf{v}. \quad (26)$$

During this excitation process, the change of the velocity on average reads

$$\Delta \mathbf{v}^{\text{ex}} = [v_- \langle \mu_{\text{ex}} \rangle(v) - v] \boldsymbol{\Omega}. \quad (27)$$

For the number of particles A which change their velocity by de-exciting processes, we obtain

$$dN_{\text{de}} = \sigma_0^{\text{de}}(v) n_{\text{B}^*} f(v\boldsymbol{\Omega}) v \, d\mathbf{v} \quad (28)$$

where the variation of the velocity is given by

$$\Delta \mathbf{v}^{\text{de}} = (v_+ \langle \mu_{\text{de}} \rangle(v) - v) \boldsymbol{\Omega}. \quad (29)$$

By multiplying dN_{ex} by $\Delta \mathbf{v}^{\text{ex}}$ and dN_{de} by $\Delta \mathbf{v}^{\text{de}}$, respectively, and integrating over \mathbf{v} , we finally obtain also the right-hand side of equation (25).

The balance equation for the energy density is established by using the weight function $v^2/2$. After appropriate manipulations, we find

$$\frac{\partial K}{\partial t} + \frac{\partial}{\partial \mathbf{r}} \cdot \mathbf{Q} - \mathbf{a} \cdot \mathbf{J} = \frac{\Delta E}{m} \left(n_{\text{B}^*} \int d\boldsymbol{\Omega} \int_0^{\infty} d\mathbf{v} v^3 \sigma_0^{\text{de}} f - n_{\text{B}} \int d\boldsymbol{\Omega} \int_{\varepsilon}^{\infty} d\mathbf{v} v^3 \sigma_0^{\text{ex}} f \right). \quad (30)$$

The integral over the collision term can be interpreted on physical grounds. The energy of the light particle changes by $-\Delta E$ due to an excitation process and by $+\Delta E$ if de-excitation occurs. Thus, by alternatively combining equations (26) and (28), we can also justify the right-hand side of equation (30). It should be noted that in the balance equations of momentum and energy the integration of the collision term with respect to v does not vanish. This means that the test particles A exchange momentum and energy with the ‘heavy’ background gas during their approach to equilibrium. Consequently, the entire momentum and energy of the particles A are not conserved. It can be shown that for the Maxwellian distribution (14), the right-hand sides of equations (25) and (30) vanish, as is to be expected.

3. The multigroup spline approximation

Since it is not possible to solve the Boltzmann equation (10) rigorously, we must introduce some approximations to find at least a numerical solution. It is useful to absorb the factor v^2 in the definition of the distribution function

$$\phi(\mathbf{r}, v\boldsymbol{\Omega}, t) = v^2 f(\mathbf{r}, v\boldsymbol{\Omega}, t). \quad (31)$$

By using the identity

$$\frac{\partial f}{\partial v} = \boldsymbol{\Omega} \frac{\partial f}{\partial v} + \frac{1}{v} \frac{\partial f}{\partial \boldsymbol{\Omega}} \quad (32)$$

the Boltzmann equation (10) transforms after some algebra into

$$\frac{\partial \phi}{\partial t} + v\boldsymbol{\Omega} \cdot \frac{\partial \phi}{\partial \mathbf{r}} + \mathbf{a} \cdot \left[\left(-\frac{2}{v} \phi + \frac{\partial \phi}{\partial v} \right) \boldsymbol{\Omega} + \frac{1}{v} \frac{\partial \phi}{\partial \boldsymbol{\Omega}} \right] + (\boldsymbol{\Omega} \times \mathbf{b}) \cdot \frac{\partial \phi}{\partial \boldsymbol{\Omega}} = \mathcal{C}[\phi] \quad (33)$$

and the collision term (11) leads to

$$\mathcal{C}[\phi] = \int d\boldsymbol{\Omega}' \left[n_{\text{B}} v \sigma^+ \phi^+ + n_{\text{B}^*} \frac{v^3}{v_-^2} \sigma \phi^- - \phi \left(n_{\text{B}} v \sigma + n_{\text{B}^*} \frac{v_+^2}{v} \sigma^+ \right) \right] \quad (34)$$

where we have used the abbreviations

$$\phi = \phi(v\boldsymbol{\Omega}) \quad \phi^+ = \phi(v_+\boldsymbol{\Omega}') \quad \phi^- = \phi(v_-\boldsymbol{\Omega}'). \quad (35)$$

To treat the velocity dependence of the newly defined distribution function ϕ , we discretize the velocity space by introducing surfaces of constant energy as boundaries of energy groups. Since the energy is given by $mv^2/2$, these surfaces are spheres with constant speed v . It is natural to start with energy zero and define the following spheres based on the excitation energy $\Delta E, 2\Delta E, \dots$ or by using the speed variable v :

$$v_0 = 0 \quad v_{v+1} = \sqrt{v_v^2 + \varepsilon^2} \quad (36)$$

where ε is given by equation (5). The length of the intervals

$$I_v = [v_{v-1}, v_v] \quad v = 1, \dots, N \quad (37)$$

is given by

$$\Delta_v = v_v - v_{v-1} \quad (38)$$

and the centres of the intervals are

$$\xi_v = \frac{v_v + v_{v-1}}{2}. \quad (39)$$

Next, we approximate the speed dependence of the distribution function ϕ between two neighbouring energy surfaces by splines of order Λ :

$$\phi(\mathbf{r}, v\boldsymbol{\Omega}, t) = \sum_{v=1}^N \phi_v(\mathbf{r}, v\boldsymbol{\Omega}, t) = \sum_{v=1}^N \chi_{I_v}(v) \sum_{\lambda=0}^{\Lambda} P_v^\lambda(v) \phi_v^\lambda(\mathbf{r}, \boldsymbol{\Omega}, t) \quad (40)$$

where $\phi_v(\mathbf{r}, v\boldsymbol{\Omega}, t)$ is the restriction of the distribution function ϕ to the interval I_v . In this representation we use the characteristic functions

$$\chi_{I_v} = \begin{cases} 1 & \text{for } v \in I_v \\ 0 & \text{elsewhere.} \end{cases} \quad (41)$$

The functions

$$P_v^\lambda(v) = \sqrt{\frac{2}{\Delta_v}} P^\lambda \left[\frac{2(v - \xi_v)}{\Delta_v} \right] \quad (42)$$

are modified Legendre polynomials (as usual P^λ denotes the common Legendre polynomials of order λ) which are defined in this manner to take advantage of the orthogonality relation within each energy group

$$\int_{I_v} P_v^\lambda P_v^l dv = \frac{2}{\Delta_v} \int_{-1}^1 P^\lambda(x_v) P^l(x_v) \frac{dv}{dx_v} dx_v = \frac{2\delta_{\lambda l}}{2l + 1} \quad (43)$$

with

$$x_v = \frac{2(v - \xi_v)}{\Delta_v}. \quad (44)$$

In this way we introduce $N \times (\Lambda + 1)$ unknowns ϕ_v^λ which depend on position \mathbf{r} , time t and angle $\boldsymbol{\Omega}$. Our main objective is now to find enough equations resulting from the Boltzmann equation to determine these unknowns.

3.1. Continuity conditions

Due to the force term of the Boltzmann equation, the distribution function must at least be continuously differentiable with respect to v . Moreover, if we demand that ϕ is M times continuously differentiable, we have to establish at the velocity knots v_v the following relations:

$$\lim_{v \rightarrow v_v^-} \phi_v^{(k)}(v_v) = \lim_{v \rightarrow v_v^+} \phi_{v+1}^{(k)}(v_v) \quad (45)$$

for $k = 0, \dots, M$ and $v = 1, \dots, N - 1$. Based on the definition of $\phi = v^2 f(v\boldsymbol{\Omega})$, the boundary conditions at the origin read

$$\phi_1(0) = 0 \quad \phi_1'(0) = 0. \quad (46)$$

If we choose the number of energy groups N large enough, we can assume at $v = v_N$ the boundary conditions

$$\phi_N^{(k)}(v_N) = 0 \quad (47)$$

for $k = 0, \dots, M - 2$. In terms of the new unknowns ϕ_v^λ , equations (45) read

$$\left. \frac{d^k}{dv^k} \sum_{\lambda=0}^{\Lambda} P_v^\lambda(v) \phi_v^\lambda \right|_{v=v_v} = \left. \frac{d^k}{dv^k} \sum_{\lambda=0}^{\Lambda} P_{v+1}^\lambda(v) \phi_{v+1}^\lambda \right|_{v=v_v} \quad k = 0, \dots, M \quad (48)$$

which finally lead to the continuity relations

$$\left(\frac{2}{\Delta_\nu}\right)^{k+\frac{1}{2}} \sum_{\lambda=k}^{\Lambda} \phi_\nu^\lambda \mathcal{N}_{k\lambda}^+ = \left(\frac{2}{\Delta_{\nu+1}}\right)^{k+\frac{1}{2}} \sum_{\lambda=k}^{\Lambda} \phi_{\nu+1}^\lambda \mathcal{N}_{k\lambda}^- \quad (49)$$

for $k = 0, \dots, M$ and $\nu = 1, \dots, N - 1$ with

$$\mathcal{N}_{k\lambda}^\pm = \frac{d^k}{dx^k} P^\lambda(x) \Big|_{x=\pm 1}. \quad (50)$$

For the boundary conditions, we finally get

$$\sqrt{\frac{2}{\Delta_1}} \sum_{\lambda=0}^{\Lambda} \phi_1^\lambda \mathcal{N}_{0\lambda}^- = 0 \quad (51a)$$

$$\left(\frac{2}{\Delta_1}\right)^{\frac{3}{2}} \sum_{\lambda=1}^{\Lambda} \phi_1^\lambda \mathcal{N}_{1\lambda}^- = 0 \quad (51b)$$

$$\left(\frac{2}{\Delta_N}\right)^{k+\frac{1}{2}} \sum_{\lambda=k}^{\Lambda} \phi_N^\lambda \mathcal{N}_{k\lambda}^+ = 0 \quad 0 \leq k \leq M - 2. \quad (51c)$$

Thus, we have $N \times (M + 1)$ independent equations, (49)–(51c), for the unknowns ϕ_ν^λ , if we demand that ϕ is M times continuously differentiable and N is the number of speed intervals.

3.2. Multigroup equations

To gain the remaining equations for ϕ_ν^λ , we multiply the Boltzmann equation (33) by weight functions P_v^l for $l = 0, \dots, L$ and integrate it over the intervals I_ν taking into account the ansatz (40). In this way, we obtain $(L + 1) \times N$ moment equations:

$$\begin{aligned} & \frac{2}{2l+1} \left(\frac{\partial \phi_\nu^l(\mathbf{r}, \boldsymbol{\Omega}, t)}{\partial t} + (\boldsymbol{\Omega} \times \mathbf{b}) \cdot \frac{\partial \phi_\nu^l(\mathbf{r}, \boldsymbol{\Omega}, t)}{\partial \boldsymbol{\Omega}} \right) + \boldsymbol{\Omega} \cdot \sum_{\lambda=0}^{\Lambda} \frac{\partial \phi_\nu^\lambda(\mathbf{r}, \boldsymbol{\Omega}, t)}{\partial \mathbf{r}} A_{\nu\lambda l} \\ & - \mathbf{a} \cdot \boldsymbol{\Omega} \sum_{\lambda=0}^{\Lambda} \phi_\nu^\lambda(\mathbf{r}, \boldsymbol{\Omega}, t) (2A_{\nu\lambda l}^{-1} + A'_{\nu\lambda l} - R_{\nu\lambda l}) + \mathbf{a} \cdot \sum_{\lambda=0}^{\Lambda} \frac{\partial \phi_\nu^\lambda(\mathbf{r}, \boldsymbol{\Omega}, t)}{\partial \boldsymbol{\Omega}} A_{\nu\lambda l}^{-1} \\ & = \sum_{\lambda=0}^{\Lambda} \int d\boldsymbol{\Omega}' [n_B \phi_{\nu+1}^\lambda(\mathbf{r}, \boldsymbol{\Omega}, t) B_{\nu\lambda l}^+(\boldsymbol{\Omega}, \boldsymbol{\Omega}') \zeta_{\nu N} \\ & + n_{B^*} \phi_{\nu-1}^\lambda(\mathbf{r}, \boldsymbol{\Omega}, t) C_{\nu\lambda l}(\boldsymbol{\Omega}, \boldsymbol{\Omega}') \zeta_{\nu 1} \\ & - \phi_\nu^\lambda(\mathbf{r}, \boldsymbol{\Omega}, t) (n_B B_{\nu\lambda l}(\boldsymbol{\Omega}, \boldsymbol{\Omega}') \zeta_{\nu 1} + n_{B^*} C_{\nu\lambda l}^+(\boldsymbol{\Omega}, \boldsymbol{\Omega}') \zeta_{\nu N})] \quad (52) \end{aligned}$$

for $\nu = 1, \dots, N$ and $l = 0, \dots, L$. To conserve the particle number, we have ensured by $\zeta_{\nu N} = 1 - \delta_{\nu N}$ that no particles are upscattered to velocities greater than v_N or downscattered from there, whereas $\zeta_{\nu 1} = 1 - \delta_{\nu 1}$ stems from the physical restrictions of the excitation and de-excitation processes. Moreover, we have introduced the following abbreviations:

$$\begin{aligned} A_{\nu\lambda l} &= \int_{I_\nu} v P_\nu^\lambda P_\nu^l dv & A_{\nu\lambda l}^{-1} &= \int_{I_\nu} \frac{1}{v} P_\nu^\lambda P_\nu^l dv \\ A'_{\nu\lambda l} &= \int_{I_\nu} P_\nu^\lambda \frac{d}{dv} P_\nu^l dv & R_{\nu\lambda l} &= P_\nu^\lambda(v_\nu) P_\nu^l(v_\nu) - P_\nu^\lambda(v_{\nu-1}) P_\nu^l(v_{\nu-1}) \end{aligned} \quad (53)$$

and

$$\begin{aligned}
 B_{v\lambda l}^+ &= \int_{I_v} P_{v+1}^\lambda(v_+) P_v^l(v) v \sigma^+ dv & C_{v\lambda l} &= \int_{I_v} P_{v-1}^\lambda(v_-) P_v^l(v) \frac{v^3}{v_-^2} \sigma dv \\
 B_{v\lambda l} &= \int_{I_v} P_v^\lambda(v) P_v^l(v) v \sigma dv & C_{v\lambda l}^+ &= \int_{I_v} P_v^\lambda(v) P_v^l(v) \frac{v_+^2}{v} \sigma^+ dv.
 \end{aligned}
 \tag{54}$$

Since we need $(\Lambda + 1) \times N$ independent equations, the relation

$$L + M + 1 = \Lambda \tag{55}$$

must be fulfilled. It will turn out that it is sufficient to choose $L = 2$ in order to ensure that the resulting system of evolution equations (52) leads to an analogous system of macroscopic equations derived in section 2.

3.3. The P_1 -approximation

Equation (52) is still of integro-differential type. To derive a system of differential equations, we expand the unknowns $\phi_v^\lambda(\mathbf{r}, \boldsymbol{\Omega}, t)$ in terms of spherical harmonics (P_N -approximation [7]).

The unit vector $\boldsymbol{\Omega} = (\sin \theta \cos \varphi, \sin \theta \sin \varphi, \cos \theta)$ is characterized by the polar angle θ and the azimuthal angle φ . Since the spherical harmonics $Y_{lm}(\theta, \varphi)$ represent an orthonormal and complete set of functions, the unknowns $\phi_v^\lambda(\boldsymbol{\Omega})$ can be represented as

$$\phi_v^\lambda(\theta, \varphi) = \sum_{l=0}^{\infty} \sum_{m=-l}^l c_{lm}^{v\lambda} Y_{lm}(\theta, \varphi) \tag{56}$$

with the coefficients

$$c_{lm}^{v\lambda} = \int_0^{2\pi} \int_{-1}^1 \phi_v^\lambda(\theta, \varphi) Y_{lm}^*(\theta, \varphi) d(\cos \theta) d\varphi. \tag{57}$$

When truncating this expansion at order two, the result can be written in the very convenient tensorial form

$$\phi_v^\lambda(\boldsymbol{\Omega}) = \frac{1}{4\pi} \left[n_v^\lambda(\mathbf{r}, t) + 3\boldsymbol{\Omega} \cdot \mathbf{j}_v^\lambda(\mathbf{r}, t) + \frac{15}{2} \left(\Omega_i \Omega_j - \frac{1}{3} \delta_{ij} \right) \mathcal{Q}_{ij}^{v\lambda}(\mathbf{r}, t) \right] \tag{58}$$

with

$$n_v^\lambda = \int \phi_v^\lambda d\boldsymbol{\Omega} \quad \mathbf{j}_v^\lambda = \int \boldsymbol{\Omega} \phi_v^\lambda d\boldsymbol{\Omega} \quad \text{and} \quad \mathcal{Q}_{ij}^{v\lambda} = \int \left(\Omega_i \Omega_j - \frac{1}{3} \delta_{ij} \right) \phi_v^\lambda d\boldsymbol{\Omega}. \tag{59}$$

Applying a P_1 -approximation to the moment equations (52) means that we set

$$\phi_v^\lambda(\boldsymbol{\Omega}) = \frac{1}{4\pi} (n_v^\lambda + 3\boldsymbol{\Omega} \cdot \mathbf{j}_v^\lambda) \tag{60}$$

by taking into account

$$\mathcal{Q}_{ij}^{v\lambda} = \int \left(\Omega_i \Omega_j - \frac{1}{3} \delta_{ij} \right) \phi_v^\lambda d\boldsymbol{\Omega} = 0. \tag{61}$$

This assumption restricts the validity of the equations to weak external fields.

Instead of inserting the approximation (60) into equation (52) and projecting it onto the basis functions 1 and $\boldsymbol{\Omega}$, we immediately project the moment equations (52) onto 1 and $\boldsymbol{\Omega}$ and refer to equations (60) and (61). This means that we multiply the moment equations by

the basis functions and integrate with respect to Ω . First, the projection of equation (52) onto 1 yields

$$\begin{aligned} & \frac{2}{2l+1} \frac{\partial}{\partial t} n_v^l(\mathbf{r}, t) + \sum_{\lambda=0}^{\Lambda} \left[A_{v\lambda l} \frac{\partial}{\partial \mathbf{r}} \mathbf{j}_v^\lambda(\mathbf{r}, t) - \mathbf{a} \cdot \mathbf{j}_v^\lambda(\mathbf{r}, t) (A'_{v\lambda l} - R_{v\lambda l}) \right] \\ &= \sum_{\lambda=0}^{\Lambda} \left[n_B \zeta_{vN} n_{v+1}^\lambda(\mathbf{r}, t) \beta_{v\lambda l}^{0+} + n_{B^*} \zeta_{v1} n_{v-1}^\lambda(\mathbf{r}, t) \gamma_{v\lambda l}^0 \right. \\ & \quad \left. - n_v^\lambda(\mathbf{r}, t) (n_B \zeta_{v1} \beta_{v\lambda l}^0 + n_{B^*} \zeta_{vN} \gamma_{v\lambda l}^{0+}) \right]. \end{aligned} \quad (62)$$

If we repeat the procedure with the weight Ω , we obtain

$$\begin{aligned} & \frac{2}{2l+1} \left(\frac{\partial}{\partial t} \mathbf{j}_v^l(\mathbf{r}, t) + \mathbf{b} \times \mathbf{j}_v^l(\mathbf{r}, t) \right) + \sum_{\lambda=0}^{\Lambda} \left[\frac{1}{3} A_{v\lambda l} \frac{\partial}{\partial \mathbf{r}} n_v^\lambda(\mathbf{r}, t) \right. \\ & \quad \left. - \frac{1}{3} \mathbf{a} n_v^\lambda(\mathbf{r}, t) (2A_{v\lambda l}^{-1} + A'_{v\lambda l} - R_{v\lambda l}) \right] = \sum_{\lambda=0}^{\Lambda} \left[n_B \zeta_{vN} \mathbf{j}_{v+1}^\lambda(\mathbf{r}, t) \beta_{v\lambda l}^{1+} \right. \\ & \quad \left. + n_{B^*} \zeta_{v1} \mathbf{j}_{v-1}^\lambda(\mathbf{r}, t) \gamma_{v\lambda l}^1 - \mathbf{j}_v^\lambda(\mathbf{r}, t) (n_B \zeta_{v1} \beta_{v\lambda l}^0 + n_{B^*} \zeta_{vN} \gamma_{v\lambda l}^{0+}) \right]. \end{aligned} \quad (63)$$

In the last equations, we introduced the constants

$$\begin{aligned} \beta_{v\lambda l}^0 &= \int B_{v\lambda l} d\Omega = \int_{I_v} P_v^\lambda(v) P_v^l(v) v \sigma_0 dv \\ \beta_{v\lambda l}^{0+} &= \int B_{v\lambda l}^+ d\Omega = \int_{I_v} P_{v+1}^\lambda(v_+) P_v^l(v) v \sigma_0^+ dv \\ \gamma_{v\lambda l}^0 &= \int C_{v\lambda l} d\Omega = \int_{I_v} P_{v-1}^\lambda(v_-) P_v^l(v) \frac{v^3}{v_-^2} \sigma_0 dv \\ \gamma_{v\lambda l}^{0+} &= \int C_{v\lambda l}^+ d\Omega = \int_{I_v} P_v^\lambda(v) P_v^l(v) \frac{v^2}{v} \sigma_0^+ dv \end{aligned} \quad (64)$$

and

$$\begin{aligned} \int \Omega B_{v\lambda l}^+ d\Omega &= \Omega' \int_{I_v} P_{v+1}^\lambda(v_+) P_v^l(v) v \sigma_1^+ dv = \Omega' \beta_{v\lambda l}^{1+} \\ \int \Omega C_{v\lambda l} d\Omega &= \Omega' \int_{I_v} P_{v-1}^\lambda(v_-) P_v^l(v) \frac{v^3}{v_-^2} \sigma_1 dv = \Omega' \gamma_{v\lambda l}^1. \end{aligned} \quad (65)$$

Substituting the ansatz (60) for ϕ_v^λ in the boundary and continuity conditions (49)–(51c) and projecting them onto 1 and Ω yields $4N \times (M+1)$ algebraic conditions for the $4N \times (\Lambda+1)$ unknowns n_v^λ , $j_{v,x}^\lambda$, $j_{v,y}^\lambda$ and $j_{v,z}^\lambda$. By means of these algebraic equations, we can express $4N \times (M+1)$ unknowns by the remaining $4N \times (L+1)$ ones (since we have $4N \times (\Lambda+1)$ unknowns and $\Lambda = M+L+1$). It appears natural to choose the first $4 \times (L+1)$ unknowns n_v^l , j_v^l , $l=0, \dots, L$ of every energy group $v=1, \dots, N$ to be independent but other choices are possible. Thus, we finally get a strongly coupled system of partial differential equations for the independent unknowns n_v^l , j_v^l with $l=0, \dots, L$ and $v=1, \dots, N$.

3.4. Macroscopic properties

Due to the spline ansatz and the P_1 -approximation, we cannot expect that the obtained distribution function fulfils exactly the original Boltzmann equation. However, depending

on the choice of the weight functions, we can ensure that the correct balance equations for the macroscopic quantities are obtained.

First we represent the macroscopic quantities, introduced in section 2, in terms of the unknowns n_v^λ , j_v^λ based on equations (16)–(20), the ansatz (40) and by using equation (59):

$$n = \int f d^3v = 2 \sum_v \sqrt{\frac{\Delta_v}{2}} n_v^0 \tag{66}$$

$$\mathbf{J} = \int \mathbf{v} f d^3v = 2 \sum_v \sqrt{\frac{\Delta_v}{2}} \left(\frac{1}{3} \frac{\Delta_v}{2} j_v^1 + \xi_v j_v^0 \right) \tag{67}$$

$$\{\mathcal{K}\}_{ij} = K_{ij} = \int v_i v_j f d^3v = \frac{2}{3} \delta_{ij} \sum_v \sqrt{\frac{\Delta_v}{2}} \left[\frac{1}{5} \frac{\Delta_v^2}{6} n_v^2 + \frac{1}{3} \xi_v \Delta_v n_v^1 + \left(\frac{\Delta_v^2}{12} + \xi_v^2 \right) n_v^0 \right] \tag{68}$$

$$K = \frac{1}{2} \text{tr} K_{ij} = \sum_v \sqrt{\frac{\Delta_v}{2}} \left[\frac{1}{5} \frac{\Delta_v^2}{6} n_v^2 + \frac{1}{3} \xi_v \Delta_v n_v^1 + \left(\frac{\Delta_v^2}{12} + \xi_v^2 \right) n_v^0 \right] \tag{69}$$

$$\begin{aligned} \mathcal{Q} = \int \frac{v^2}{2} \mathbf{v} f d^3v = \sum_v \sqrt{\frac{\Delta_v}{2}} \left\{ \frac{1}{7} \frac{\Delta_v^3}{20} j_v^3 + \frac{1}{5} \frac{\Delta_v^2}{2} \xi_v j_v^2 + \frac{1}{3} \left[\frac{3}{5} \left(\frac{\Delta_v}{2} \right)^3 + \frac{3}{2} \xi_v^2 \Delta_v \right] j_v^1 \right. \\ \left. + \left(\frac{\Delta_v^2}{4} \xi_v + \xi_v^3 \right) j_v^0 \right\}. \end{aligned} \tag{70}$$

Equation (66) implies that we must multiply equation (62) for $l = 0$ by $\sqrt{\Delta_v/2}$ and sum the resulting equations over v in order to check if the conservation of the particle number is incorporated in the moment equations (62) and (63). Finally, this calculation leads to

$$2 \frac{\partial}{\partial t} \sum_v n_v^0 \sqrt{\frac{\Delta_v}{2}} + 2 \frac{\partial}{\partial \mathbf{r}} \sum_v \sqrt{\frac{\Delta_v}{2}} \left(\frac{1}{3} \frac{\Delta_v}{2} j_v^1 + \xi_v j_v^0 \right) = 0 \tag{71}$$

which is exactly the continuity equation, bearing in mind equations (66) and (67).

Next, we derive the equation of momentum transport. The structure of equation (25) and the definition of the current density, equation (67), suggest that we must multiply equation (63) for $l = 0$ by $\xi_v \sqrt{\Delta_v/2}$ and add it to equation (63) for $l = 1$ multiplied by $(\Delta_v/2)^{3/2}$ and sum the resulting equation over all energy groups. In this way we get

$$\begin{aligned} 2 \frac{\partial}{\partial t} \sum_v \sqrt{\frac{\Delta_v}{2}} \left(\frac{1}{3} \frac{\Delta_v}{2} j_v^1 + \xi_v j_v^0 \right) + \mathbf{b} \times 2 \sum_v \sqrt{\frac{\Delta_v}{2}} \left(\frac{1}{3} \frac{\Delta_v}{2} j_v^1 + \xi_v j_v^0 \right) \\ + \frac{2}{3} \frac{\partial}{\partial \mathbf{r}} \sum_v \sqrt{\frac{\Delta_v}{2}} \left[\frac{1}{5} \frac{\Delta_v^2}{6} n_v^2 + \frac{1}{3} \xi_v \Delta_v n_v^1 + \left(\frac{\Delta_v^2}{12} + \xi_v^2 \right) n_v^0 \right] - 2\mathbf{a} \sum_v \sqrt{\frac{\Delta_v}{2}} n_v^0 \\ = n_B \int_\epsilon^{v_N} dv v \sigma_0^{\text{ex}} (v - \langle \mu_{\text{ex}} \rangle - v) \int d\Omega \Omega \phi \\ + n_{B^*} \int_0^{v_{N-1}} dv v \sigma_0^{\text{de}} (v + \langle \mu_{\text{de}} \rangle - v) \int d\Omega \Omega \phi. \end{aligned} \tag{72}$$

Comparing this result with the original momentum transport equation (25), we see that they only differ in the upper bounds of the integrals, which is caused by the finite number of energy groups.

In addition, the balance equation of energy density is hidden in the moment equations. The definition of the energy density per unit mass (69) implies that we proceed in the following way:

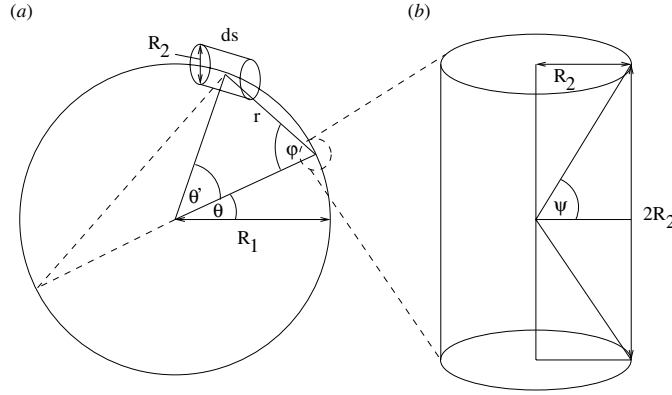


Figure 1. Geometry used for the calculation of the self-consistent field (a). For $R_1 \gg R_2$ the neighbourhood of $\theta' = 0$ is replaced by a cylinder of height $2R_2$ (b).

- Taking the moment equations (62) for $l = 0, 1, 2$ and multiplying them by the following factors $l = 0 : \left(\frac{\Delta_v^2}{12} + \xi_v^2\right)$, $l = 1 : \xi_v \Delta_v$, $l = 2 : \frac{\Delta_v^2}{6}$;
- then adding the resulting equations and multiplying them by the common factor $\frac{1}{2}\sqrt{\frac{\Delta_v}{2}}$;
- and finally summing over all energy groups.

This results in

$$\begin{aligned}
 & \sqrt{\frac{\Delta_v}{2}} \frac{\partial}{\partial t} \sum_v \left[\frac{1}{5} \frac{\Delta_v^2}{6} n_v^2 + \frac{1}{3} \xi_v \Delta_v n_v^1 + \left(\frac{\Delta_v^2}{12} + \xi_v^2 \right) n_v^0 \right] + \frac{\partial}{\partial r} \cdot \sum_v \sqrt{\frac{\Delta_v}{2}} \left\{ \frac{1}{7} \frac{\Delta_v^3}{20} j_v^3 + \frac{1}{5} \frac{\Delta_v^2}{2} \xi_v j_v^2 \right. \\
 & \quad \left. + \frac{1}{3} \left[\frac{3}{5} \left(\frac{\Delta_v}{2} \right)^3 + \frac{3}{2} \xi_v^2 \Delta_v \right] j_v^1 + \left(\frac{\Delta_v^2}{4} \xi_v + \xi_v^3 \right) j_v^0 \right\} \\
 & \quad - 2a \cdot \sum_v \sqrt{\frac{\Delta_v}{2}} \left(\frac{1}{3} \frac{\Delta_v}{2} j_v^1 + \xi_v j_v^0 \right) \\
 & = - \frac{\Delta E}{m} n_B \int d\Omega \int_{\varepsilon}^{v_N} dv v \sigma_0^{\text{ex}} \phi + \frac{\Delta E}{m} n_{B^*} \int d\Omega \int_0^{v_N} dv v \sigma_0^{\text{de}} \phi. \quad (73)
 \end{aligned}$$

Thus, we have again discovered the balance equation for the energy density (30).

The results reveal that we must at least choose $L = 2$ to ensure the conservation of the particle number and a physically correct treatment of the transport of momentum and energy by our moment equations. By using Legendre polynomials of higher orders, we can also recover any other macroscopic equation, as e.g. the heat flow equation. Hence, we can improve the relevance of our physical description which, however, entails an increasingly higher number of differential equations.

4. Numerical simulations

In the previous section, we deduced a system of evolution equations (62) and (63) for charged particles diffusing through a host medium of two-level atoms based on a multigroup spline P_1 -approximation. To demonstrate the applicability of the underlying method, we consider the transport within a thin torus with the radii R_1 and R_2 (figure 1(a)). If we suppose that $R_1 \gg R_2$, we can approximately assume that the velocity distribution depends only on the

polar angle θ . We further assume that only tangential electric forces act on the charged test particles. A finite radius $R_2 \neq 0$ is necessary to avoid singularities of the electric field strength. Moreover, the tangential electric force is considered to be constant over the cross section of the torus and given by its actual value at $R_2 = 0$. This means that we deal with a one-dimensional transport problem in real space, where periodic boundary conditions with respect to the angle variable θ apply:

$$\phi(\theta, v, t) = \phi(\theta + 2\pi, v, t). \quad (74)$$

For all simulations, we assume that the differential excitation cross section is given by

$$\sigma_{\text{ex}} = \begin{cases} 0 & \text{for } v < \varepsilon \\ 1 & \text{for } v \geq \varepsilon. \end{cases} \quad (75)$$

By virtue of microreversibility (6), the cross section of de-excitation reads

$$\sigma_{\text{de}} = 1 + \left(\frac{\varepsilon}{v}\right)^2. \quad (76)$$

Furthermore, we require that the distribution function is continuously differentiable, which means that we set $M = 1$ in our simulations.

4.1. The self-consistent electric field

Since we consider charged test particles, we must take into account the time-dependent self-consistent electric field $\mathbf{E}_{\text{self}}(\theta, t)$ due to the Maxwell equation

$$\nabla \cdot \mathbf{E}_{\text{self}} = \frac{\rho}{\varepsilon_0} \quad (77)$$

corresponding to the charge density

$$\rho(\theta, t) = e(n_{\text{B}} + n_{\text{B}^*} - n(\theta, t)).$$

The last equation is based on the assumption that the heavy background particles are positive ions, whereas the test particles are negatively charged and the particle density of the background particles is spatially homogeneous. Moreover, dynamical electromagnetic effects are neglected.

Integrating equation (77) yields the tangential component of the electric field at $\theta = 0$:

$$E_{\text{self}}(0) = \int_{\text{torus}} \frac{\rho(\theta') \sin \varphi}{4\pi \varepsilon_0 r^2} dV, \quad (78)$$

where ε_0 denotes the dielectric constant, r is the distance between field point and source point and $\varphi = (\pi - \theta')/2$. It should be noted that the integrand is singular for $r = 0$, which would result in an infinitely strong electric field in the case of a one-dimensional volume element dV . However, we avoid this problem by assuming a torus with $R_2 \neq 0$. Since we suppose $R_1 \gg R_2$, we can approximate the torus in the neighbourhood of $\theta' = 0$ by a cylinder of height $2R_2$ (figure 1(b)). This enables us, after some algebra, to evaluate the tangential electric field component E_{cyl} at $\theta = 0$ caused by the charge density within this cylinder by taking into account the exact distance r between source point and field point in

equation (78):

$$E_{\text{cyl}}(0) = \frac{R_2}{2\varepsilon_0} \int_{-\frac{\pi}{4}}^{\frac{\pi}{4}} \rho(\vartheta) (\sin \psi - \text{sign } \psi) \frac{1}{\cos^2 \psi} d\psi \quad (79)$$

with $\vartheta = \frac{R_2 \tan \psi}{R_1}$. To estimate the contribution of the rest of the torus to the tangential electric field at $\theta = 0$, we approximate the distance r in equation (78) for each volume element $dV = R_2^2 \pi ds$ by $r = 2R_1 \cos \varphi$, which results in

$$E_{\text{rest}}(0) = -\frac{R_2^2}{8\varepsilon_0 R_1} \int_{-\frac{\pi}{2}+\delta}^{\frac{\pi}{2}-\delta} \frac{\rho(\pi - 2\varphi) \sin \varphi}{\cos^2 \varphi} d\varphi \quad (80)$$

where $\delta = \frac{R_2}{2R_1}$ and $ds = 2R_1 d\varphi$. In order to obtain the tangential component of the electric field at an arbitrary position θ , we simply rotate the coordinate system by this angle θ , which leads to

$$E_{\text{rest}}(\theta) = -\frac{R_2^2}{8\varepsilon_0 R_1} \int_{-\frac{\pi}{2}+\delta}^{\frac{\pi}{2}-\delta} \frac{\rho(\pi - 2\varphi + \theta) \sin \varphi}{\cos^2 \varphi} d\varphi \quad (81)$$

and

$$E_{\text{cyl}}(\theta) = \frac{R_2}{2\varepsilon_0} \int_{-\frac{\pi}{4}}^{\frac{\pi}{4}} \rho(\vartheta + \theta) (\sin \psi - \text{sign } \psi) \frac{1}{\cos^2 \psi} d\psi. \quad (82)$$

Therefore, the whole self-consistent electric field is given by

$$E_{\text{self}}(\theta) = E_{\text{rest}}(\theta) + E_{\text{cyl}}(\theta). \quad (83)$$

In the numerical simulations the following algorithmic pattern is used. We start with a given initial distribution function of the test particles and evaluate the corresponding electric field by means of equations (81)–(83). Then, we solve the group equations (62) and (63) under the influence of this fixed initial electric field for a short period of time Δt . Using the newly evaluated distribution function, we recalculate the self-consistent electric field and repeat the whole procedure to approach equilibrium.

4.2. Results of the simulations

It is useful to define natural units. We choose the unit of mass such that the mass of particle A equals 1. This means, if particles A are assumed to be electrons that $m_A = 1 \simeq 9.1096 \times 10^{-31}$ kg. The energy is measured in units of $k_b T$. Considering $T = 300$ K, leads to $E = 1 \simeq 25.85$ meV. The particle density of realistic systems is of order 10^{21} particles per m^3 . By setting the unit length $l = 1 \simeq 10^{-7}$ m, we get $n = 1 \simeq 10^{21} \text{m}^{-3}$. These definitions are only consistent if we change the unit of time to $t = 1 \simeq 1.48 \times 10^{-12}$ s. Moreover, we measure the charge in terms of the elementary charge $e = 1 \simeq 1.60219 \times 10^{-19}$ As. The factor for converting the electric field is then given by $E = 1 \simeq 258512 \text{V m}^{-1}$. For all simulations, we fix the parameters to $L = 2$, $N = 10$, $\varepsilon = 1.9$ and $n_B = 3$, which is consistent with equation (55) if we choose $\Lambda = 4$.

To show how fast equilibrium is approached, we first assume that the particle density is constant throughout the torus. Figure 2 shows the temporal evolution of a given initial distribution function. We finally obtain at $t = 0.5$ the expected Maxwellian as displayed in figure 3. The number of occurring oscillations of the non-equilibrium distribution function at $t = 0.1$ is directly related to the group number. This can be seen by comparing figure 3 with figure 4, where the same relaxation process is shown, however, by using only four

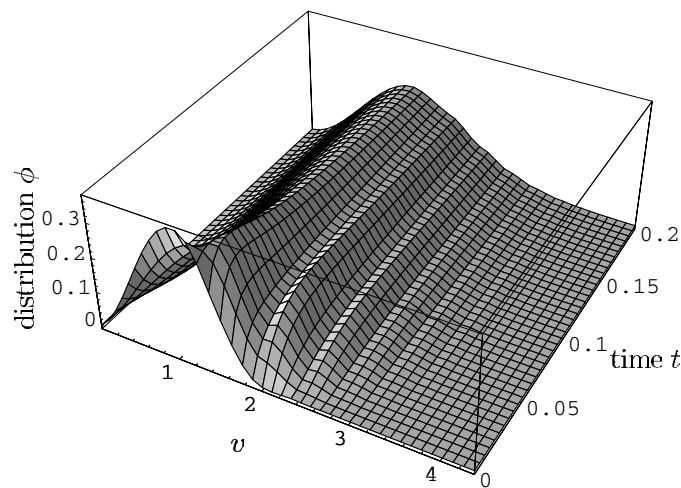


Figure 2. The relaxation of a given initial distribution function to a Maxwellian. The plot shows the distribution ϕ versus speed v and time t .

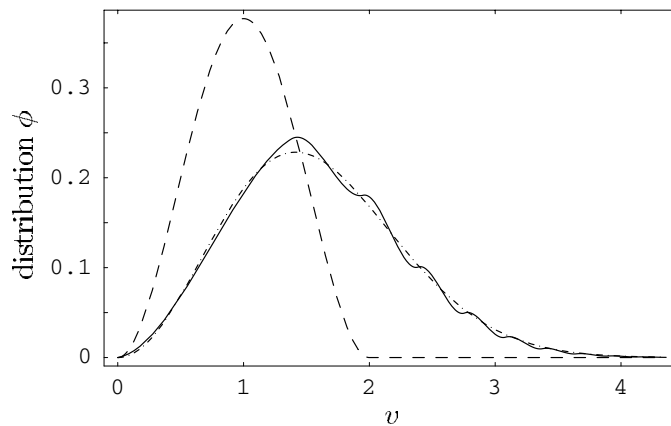


Figure 3. The distribution ϕ at different times (--- $t = 0$, — $t = 0.1$ and - · - $t = 0.5$). The distribution function for $t = 1$ coincides with the theoretically expected Maxwellian for $T = 300$ K.

groups ($N = 4$). The oscillations seem to be a consequence of the spline approximation used combined with the strict adherence to the balance equation of momentum and energy. They do not appear in that case only particle conservation is ensured by the multigroup equations. Moreover, investigations using ordinary polynomials as basis functions lead to the same numerical result, apart from the fact that the oscillations do not vanish in the approach to equilibrium. Using a finer discretization scheme, as given by the excitation energy ΔE , would reduce the amplitude of the oscillations, but has the drawback that neighbouring energy groups decouple. (Inelastic scattering of particles into neighbouring groups is then impossible.) The evolution of the energy density K is illustrated in figure 5. Since the initial distribution has more slow particles than the final Maxwellian, the energy

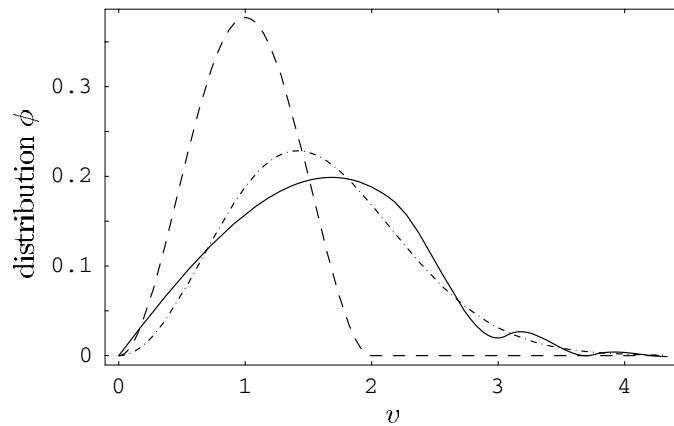


Figure 4. The distribution ϕ at different times ($---$ $t = 0$, $—$ $t = 0.1$ and $- \cdot -$ $t = 0.5$) by using four groups instead of ten (compare figure 3).

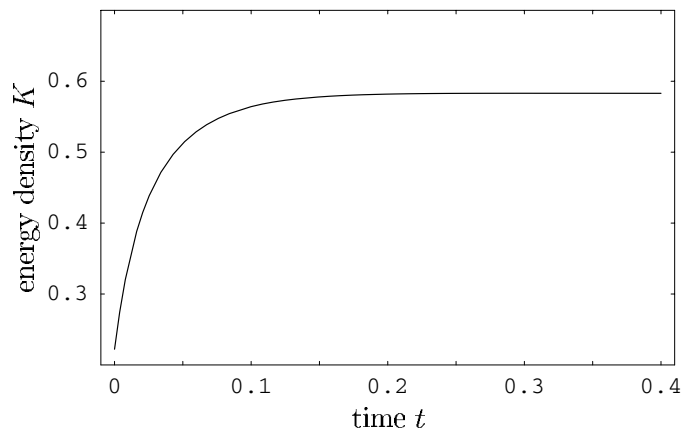


Figure 5. Temporal relaxation of the energy density K .

density increases temporally. The conservation of the particle number which represents a criterion for the quality of the numerical calculations is fulfilled with high accuracy in our simulations.

Next, we investigate the diffusion of particles caused by a spatially varying particle density in the torus. The initially parabolic-shaped particle density n tends to a spatially constant density, which can be seen in figures 6 and 7. Figure 8 shows that the diffusion is slowed down if one disregards the self-consistent electric field.

Finally, we study the impact of a harmonic external electric field, $E_{\text{ex}} = A \cos(\omega t)$, which is switched off at time $t_E = 40$ with $A = 0.002$ and $\omega = 2\pi/19$. Figure 9 shows the expected appearance of a sinusoidal current density in the torus. After switching off the electric field, the current is strongly slowed down by inelastic collisions of the particles.

By applying stronger electric fields $E > 5 \text{ kV m}^{-1}$, we observe negative values for the distribution function, which means that the P_1 -approximation is no longer valid. This can be

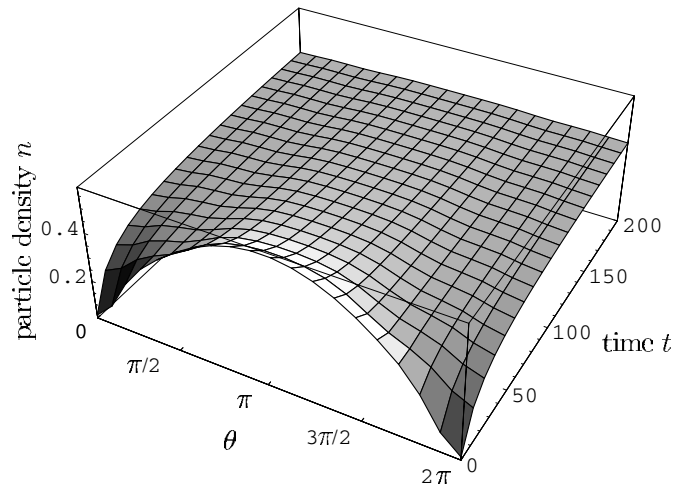


Figure 6. Spatio-temporal evolution of the particle density n in a torus.

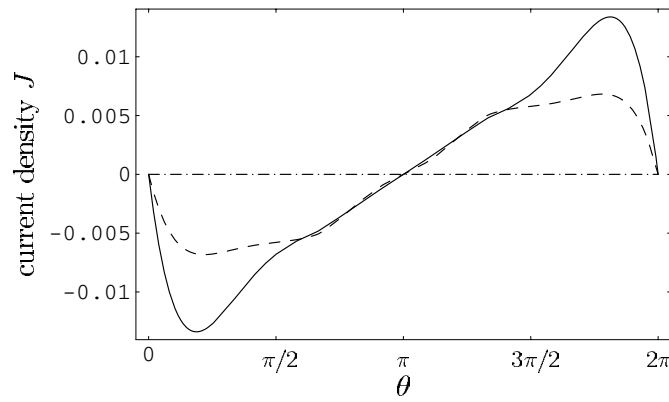


Figure 7. The current density J versus the angle θ at several times (— $t = 1$, --- $t = 50$ and - · - $t = 200$) in a torus.

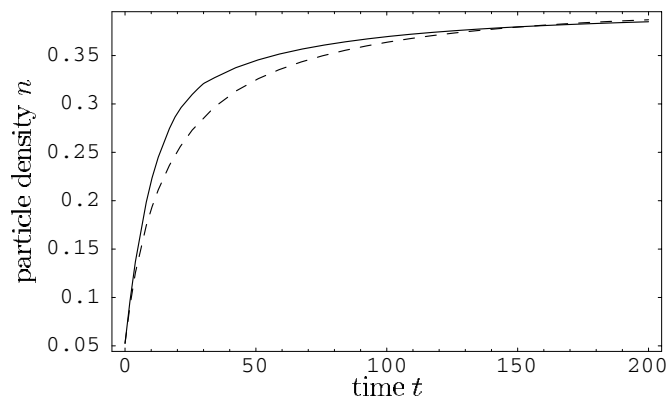


Figure 8. The temporal evolution of the particle density n at $\theta = 0$ for the cases of regarding (—) and disregarding (---) the self-consistent electric field, respectively.

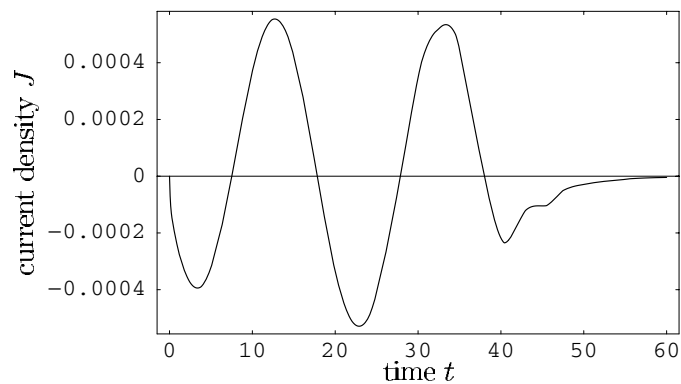


Figure 9. The current density at point $\theta = \pi/2$ versus time t . The harmonic external electric field is switched off at $t_E = 40$.

repaired by considering higher orders of the P_N -approximation, which, however, prolongate the calculations.

5. Conclusion

This paper treats an extended linear Boltzmann equation governing the distribution function of charged particles colliding inelastically with resting heavy background particles. By establishing a multigroup spline P_1 -approximation, the Boltzmann equation is transformed into a system of differential equations. It is ensured that these model equations lead to the correct balance equations for the macroscopic quantities. The system of differential equations is solved numerically for the geometry of a thin torus by taking into account the self-consistent electric field and external forces. The numerical experiments show that the validity of the spline P_1 -approximation used for the distribution function is limited to weak external forces. An improvement is possible by using higher-order P_N -approximations; however, this extends the calculations.

Acknowledgment

This work was supported by the Fonds zur Förderung der wissenschaftlichen Forschung, Vienna, under contract number P14669-TPH.

References

- [1] Lapidus L and Pinder G F 1982 *Numerical Solutions of Partial Differential Equations in Science and Engineering* (New York: Wiley)
- [2] Duderstadt J and Martin W 1979 *Transport Theory* (New York: Wiley)
- [3] Caraffini G L, Ganapol B D and Spiga G 1995 A multigroup approach to the non-linear extended Boltzmann equation *Nuovo Cimento D* **17** 129–42
- [4] Koller W 2000 Semi-continuous and multigroup models in extended kinetic theory *PhD Thesis* Technical University, Graz p 135
- [5] Majorana A 1991 Space homogenous solutions of the Boltzmann equation describing electron phonon interactions in semiconductors *Transp. Theory. Stat. Phys.* **20** 261–79
- [6] Rossani A and Spiga G 1998 Kinetic theory with inelastic interactions *Transp. Theory. Stat. Phys.* **27** 273–83
- [7] Bell G and Glasstone S 1970 *Nuclear Reactor Theory* (New York: Van Nostrand Reinhold)